

Timing and spectral properties of PSR B0540–69 observed with BeppoSAX

T. Mineo¹, G. Cusumano¹, E. Massaro², L. Nicastro¹, A.N. Parmar³, and B. Sacco¹

¹ Istituto di Fisica Cosmica ed Applicazioni all'Informatica CNR, Via U. La Malfa 153, I-90146 Palermo, Italy

² Istituto Astronomico, Unita' GIFCO Roma-1, Universita' "La Sapienza", Via Lancisi 29, I-00161 Roma, Italy

³ Astrophysics Division, Space Science Department of ESA, ESTEC, Post box 299, 2200 AG Noordwijk, The Netherlands

Received 4 November 1998 / Accepted 25 January 1999

Abstract. BeppoSAX observed PSR B0540–69 on 1996 October 25–26 during the Science Verification Phase. The pulsar, detected by the imaging LECS and MECS instruments (0.1–10 keV), shows a characteristic nearly sinusoidal pulse structure with a minor structure on the left side of the maximum. By combining the BeppoSAX measurements with earlier ASCA results we derived a low value of the braking index of 2.10 ± 0.10 . We also investigate the X-ray spectral distribution of the pulsed emission in the energy band (2–10) keV. We find that it can be well represented by a single absorbed power-law with energy index of 0.76 ± 0.14 and $N_{\text{H}} = (3.6 \pm 0.7) \times 10^{21} \text{ cm}^{-2}$.

Key words: stars: neutron – stars: pulsars: general – stars: pulsars: individual: PSR B0540–69 – X-rays: stars

1. Introduction

PSR B0540–69 was discovered in the soft X-rays by Einstein (Seward et al. 1984) in the Large Magellanic Cloud. Pulsations at optical frequencies were soon discovered (Middleditch & Pennypacker 1985) with a mean pulsed magnitude of 22.5. Despite the large spin down luminosity of $\sim 10^{38} \text{ erg s}^{-1}$, PSR B0540–69 is a faint radio source and pulsed signals in the radio band were first observed only in 1989–90 (Manchester et al. 1993).

PSR B0540–69 is one of the youngest rotation powered pulsars. With a period of about 50 ms and a large period derivative of $4.79 \times 10^{-13} \text{ s s}^{-1}$ comparable to that of the Crab pulsar, it has spin down age of about 1500 years. The pulse shape, at X and optical wavelengths, is broad, almost sinusoidal. Seward et al. (1984) observed a slight bifurcation at the top of the broad pulse, but it was not always detected in subsequent observations. Several estimates of the braking index n have been reported in the literature (see Boyd et al. 1995 for a compilation of earlier results) ranging from 2.01 ± 0.02 (Manchester & Peterson 1989; Nagase et al. 1990) to 2.74 ± 0.10 (Ögelman & Hasinger 1990). The most recent evaluation, based on a detailed analysis of GINGA observations, is 2.08 ± 0.02 (Deeter et al. 1998). In

this paper we describe the results of a BeppoSAX observation of this source. In particular, we verify the braking index estimates with our timing and study the spectral distribution of the pulsed component.

2. Observation and data reduction

PSR B0540–69 was observed on October 1996 25–26 by the Narrow Field Instruments (NFIs) onboard BeppoSAX satellite (Boella et al. 1997a) during the Science Verification Phase. The NFIs consist of four coaligned instruments: the Low Energy Concentrator Spectrometer (LECS) operating in the energy range (0.1–10) keV (Parmar et al. 1997), the Medium Energy Concentrator Spectrometer (MECS) operating in the (1–10) keV (Boella et al. 1997b), the High Pressure Gas Scintillation Proportional Counter (HPGSPC) operating in the (4–120) keV (Manzo et al. 1997) and the Phoswich Detector System (PDS) operating in the (15–300) keV energy band (Frontera et al. 1997). In the following analysis we will use the data from the LECS and MECS only. These are both imaging instruments with a field of view of $37'$ and $56'$ respectively. At the observation epoch all the MECS detectors were operating so that its effective area was about three time larger than that of the LECS in the overlapping band. The angular resolution is about $1/2$ at 6 keV for both instruments. During the observations of PSR B0540–69 the instruments operated in direct mode transmitting to ground information on each individual photon. Standard procedures and selection criteria were applied on observation data to avoid the South Atlantic Anomaly, solar, bright Earth and particle contaminations¹. The total duration of the observation was 71 379 s and the net exposure times were 20 329 s for the LECS, 46 700 s for the MECS. Data in the LECS and MECS were selected within a circular region centered at the source and $4'$ of radius. This selection, that contains the 90% of the source signal in the MECS and 90% of the (0.1–2.0) keV flux in LECS, reduced strongly the contamination caused by the intense X-ray source LMC X-1, only $26/4$ far from PSR B0540–69. The LECS and MECS events were reduced using the SAXDAS v.1.1.0 package.

¹ see <http://www.sdc.asi.it/software/cookbook> as a reference about the data analysis software and reduction procedures.

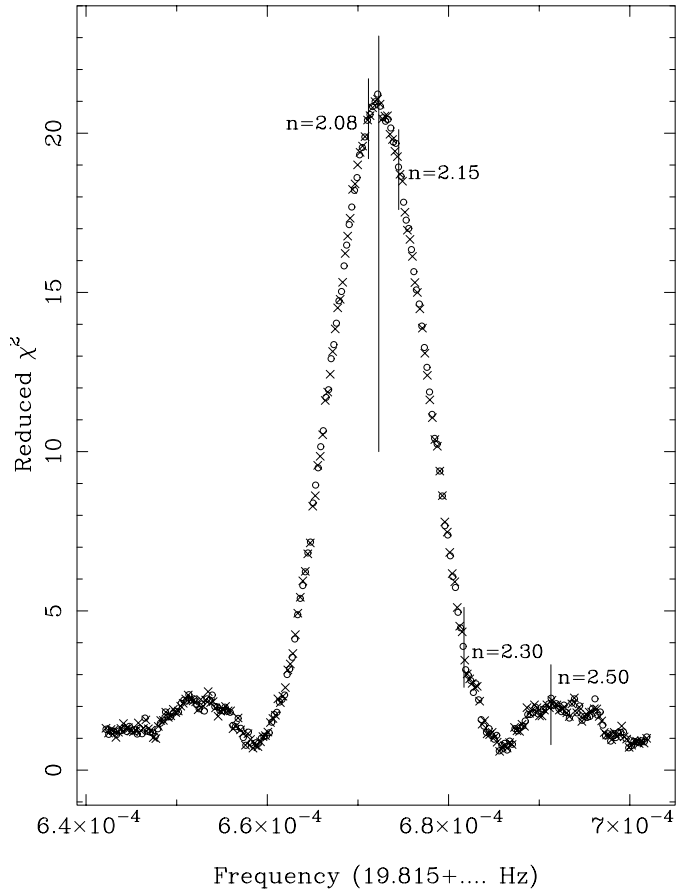


Fig. 1. The periodogram of PSR B0540–69 for the (1–10) keV (MECS) data: crosses and open circle are the χ^2 values when the frequency derivative is included or not in the folding, respectively. The long vertical bar indicates the peak centre, the short ones indicate the expected pulsar frequencies for some values of the braking index.

The UTC arrival time of all selected events were first converted to the Solar System Barycenter using the (J2000) pulsar position $\alpha = 05^{\text{h}}40^{\text{m}}11^{\text{s}}.03$ and $\delta = -69^{\circ}19'57''.5$ (Gouiffes et al. 1992). The pulsed signal was searched by applying the folding technique to the MECS data series because of the best S/N ratio. Since recent ephemeris were not available, the period was optimized by a χ^2 maximization starting from a value of the pulsar period and first derivative estimated by a simple extrapolation from the data of Boyd et al. (1995). The period step size used in this search was 1.4×10^{-9} s. We fixed the reference epoch for the folding at MJD 50 382.32099, the central time of the observation.

3. Results

3.1. Timing and braking index

The plot of the χ^2 vs the pulsar frequency for the BeppoSAX observation is shown in Fig. 1. It has a prominent and smooth maximum, much higher than the noise level. The two symbols indicate the χ^2 values computed assuming the first frequency derivative equal to zero and to -1.88×10^{-10} Hz s $^{-1}$ (Boyd

et al. 1995). No significant difference is apparent, confirming that this parameter does not affect the frequency estimate because of the reference epoch adopted in folding the data. We applied a parabolic fit to evaluate the central value of this peak and its uncertainty. Several fits were computed over a set of different frequency intervals and the median of the distribution of these values was taken as the best estimate of the pulsar frequency while the half range of the distribution as an estimate of the frequency uncertainty. We obtained the value $\nu = 19.8156723 \pm 0.0000004$ Hz. To compare this result with the recent analysis of Deeter et al. (1998), we extrapolated their data frequency at the epoch of the BeppoSAX observation. We integrated the braking law

$$\dot{\nu} = -a\nu^n \quad (1)$$

with a constant n and obtained

$$\nu(t) = \nu_0^{n/(n-1)} [\nu_0 - \dot{\nu}_0(n-1)(t-t_0)]^{1/(1-n)} \quad (2)$$

where t_0 is the reference epoch (for the GINGA observations is 47 700.0 MJD), and ν_0 and $\dot{\nu}_0$ are the pulsar frequency and the first derivative at this epoch. Using for the braking index the value $n = 2.08$ (Deeter et al. 1998) we obtained for the BeppoSAX observation epoch $\nu_{\text{ex}} = 19.81567116 \pm 0.00000016$ Hz, quite close but smaller than the central frequency of the χ^2 peak (Fig. 1). A precise agreement would require $n = 2.104$. Using much greater n values we find a larger and larger disagreement: the expected frequencies for $n = 2.30$ and 2.50 lie well far from the maximum, as shown in Fig. 1. The estimate of the uncertainty on n is not simple because of systematic effects, mainly the unknown true pulse shape. Using the error on the frequency given above, we found a very small value of the uncertainty (0.009). In principle, however, it is not sure that the actual pulsar frequency is exactly the one corresponding to the χ^2 maximum; we checked that phase histograms at frequencies within the peak also give sinusoidal pulse profiles not very different from the central one (this could be the source of the timing noise of frequency measurements which led to the span of the n estimates). In any case, the real frequency cannot lie very far from the peak centre and therefore the quite conservative estimate of $n = 2.10 \pm 0.10$ must be considered reliable. This analysis confirms, therefore, the low value of the braking index of this young pulsar over a 2 682 day time lag.

We evaluated also the frequency derivative by analysing a couple of recent observations from the ASCA public archive for which high telemetry data are available. We choose the pointings closest in time to the epoch of the BeppoSAX pointing and precisely those at the MJD epochs 49 626.068 (sequence 22004000) and 49 636.35 (sequence 22004020). Using again the folding method as above, we obtained the two frequencies 19.82796324 and 19.8277942 Hz, respectively. Again these values agree well with those computed by Eq. (2). The frequency derivative between the ASCA and BeppoSAX pointings was estimated by means of three point linear fit and resulted $\dot{\nu} = -1.88085 \times 10^{-10}$ Hz s $^{-1}$. A check with the value expected from the Deeter et al. (1998) ephemeris can be made by Eqs. (1) and (2): again a value consistent with the measured one

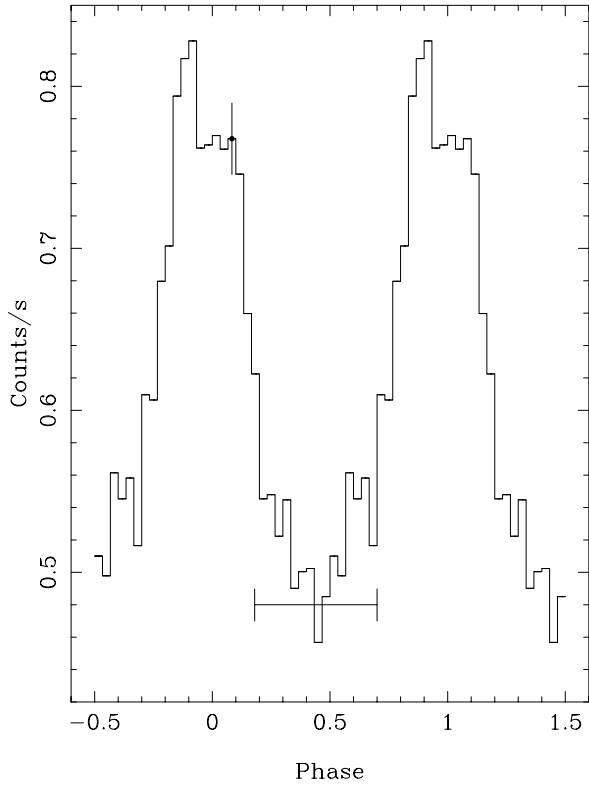


Fig. 2. The pulse profile of PSR B0540–69 in the (1–10) keV energy range (MECS). The zero phase is arbitrarily chosen at 50 382.32099058 MJD. The $\pm 1 \sigma$ uncertainty is shown. The off-pulse interval used for the spectral analysis is also reported.

is obtained. All the resulting time parameters are summarized in Table 1.

3.2. The pulse profile

The pulse profile of PSR 0540–69 in the whole MECS energy range (1.0–10 keV) is shown in Fig. 2; the zero phase is arbitrarily chosen at 50 382.32099058 MJD. The profile has the nearly sinusoidal shape observed since the first detection, however, we do not find evidence of the slight bifurcation at the top of the peak described by Seward et al. (1984). If a minor structure is present, it may be the peak just on the left side of the maximum. In Fig. 3a,b the profiles in the two energy ranges (1.6–4.0) and (4.0–10) keV are shown: the shape of the main peak is the same in both data sets, but the small peak appears only in the lower energy phase histogram.

Fig. 4 shows the pulse profile derived by the LECS (0.1–2.0 keV) using the best frequency estimate obtained from MECS analysis. The statistics are poorer than in the MECS data, but signals with the right shape and phase are detectable. Notice that the double structure at the peak top seems more evident suggesting that it could be more prominent at lower energies. The S/N ratio of the LECS profile, however, is too low to reach any firm conclusion about the significance of these features. They are not so evident in the ROSAT master pulse profile obtained by combining many observations spanning about three years

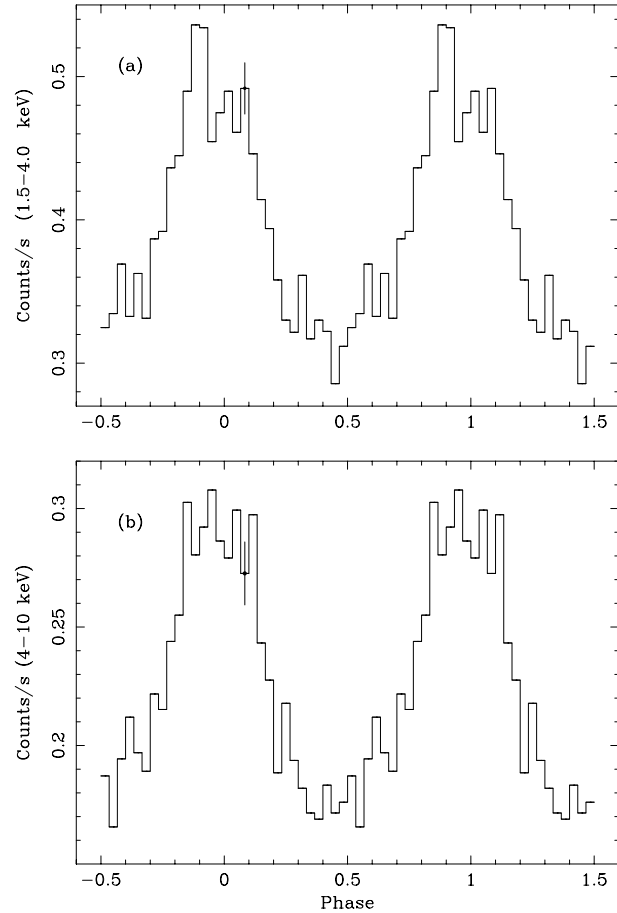


Fig. 3a and b. The pulse profile of PSR B0540–69 in the (1.6–4) keV **a** and (4–10) keV **b** energy ranges.

Table 1. Timing parameter estimates for PSR 0540–69

Parameter	Value ^a
Epoch (MJD)	50 382.32099
ν	19.8156723(4)
$\dot{\nu}$	$-1.88085(4) \times 10^{-10}$
Braking index	2.10(10)

^a Values in parentheses are the 1σ uncertainties in the last quoted digits

(Eikenberry et al. 1998). Notice also that the possible structures in the off-pulse segment of our profile do not match precisely the phases of the small peaks visible in the master profile of ROSAT and therefore we think that they should be statistical fluctuations.

The PDS data, at energies greater than 13 keV, do not show any significant pulsed signal: only an excess smaller than 2 standard deviations is present in the periodogram at the MECS frequency.

3.3. The energy spectrum

The study of the energy spectral distribution of the whole source is not simple because the local background has an energy de-

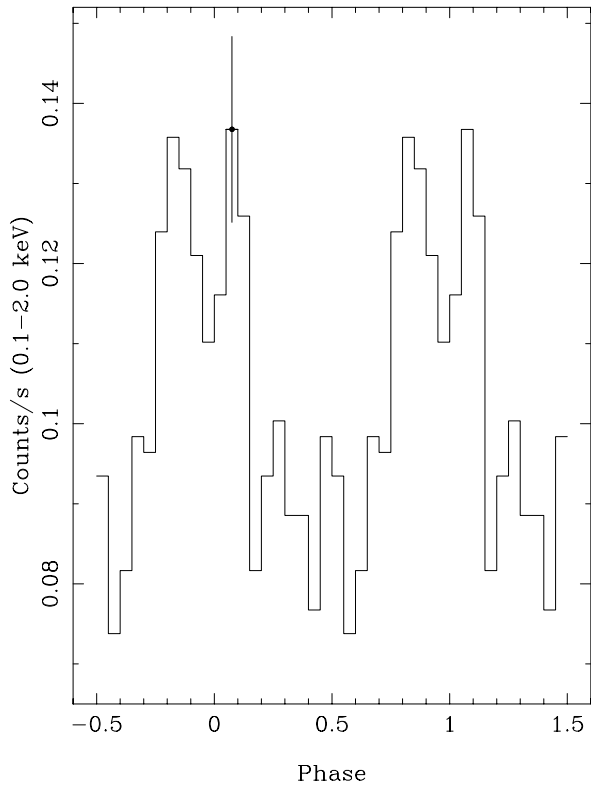


Fig. 4. The pulse profile of PSR B0540–69 in the low energy band (0.1–2.0 keV) of the LECS.

pendence below 1 keV variable with position and therefore we decided to limit our analysis only to photons above this energy. For the pulsed emission this problem is not present because the background is automatically subtracted with the off-pulse signal; the only problem arises from the broad peak shape that does not allow a clear definition of the off-pulse interval. The phase averaged spectrum of the (1.0–10 keV) LECS and MECS data can be fitted well by a power-law with low energy absorption: the N_{H} value is $(3.6 \pm 0.7) \times 10^{21} \text{ cm}^{-2}$ and the photon spectral index (from the MECS data only) is 1.94 ± 0.03 , with a reduced $\chi^2 = 0.98$ (145 dof). Both these values are in agreement within their uncertainties with those of Finley et al. (1993) obtained from the (0.1–2.4) keV ROSAT data.

To evaluate the pulsed spectrum we assumed the off-pulse in the phase interval (0.18–0.70) - with the phase values of Fig. 2 - in order to limit the pulsed signal to the prominent core of the peak. Fixing the low energy absorption to the value obtained for the total spectrum, the power-law spectrum gives again a good fit to the data (Fig. 5). The resulting photon spectral index is 1.76 ± 0.14 and the unabsorbed flux in the energy interval (2.0–10) keV is $(5.87 \pm 0.22) \times 10^{-12} \text{ erg cm}^{-2} \text{ s}^{-1}$. From the LECS data we derive an estimate of the (0.1–2.0 keV) unabsorbed pulsed flux of $(7.1 \pm 1.0) \times 10^{-12} \text{ erg cm}^{-2} \text{ s}^{-1}$. The ROSAT results (Finley et al. 1993) gave a flatter spectrum of the “pulsed” component with respect to the nebular one. Our low energy flux is somewhat larger than the one given by these authors, but again within the measured uncertainties.

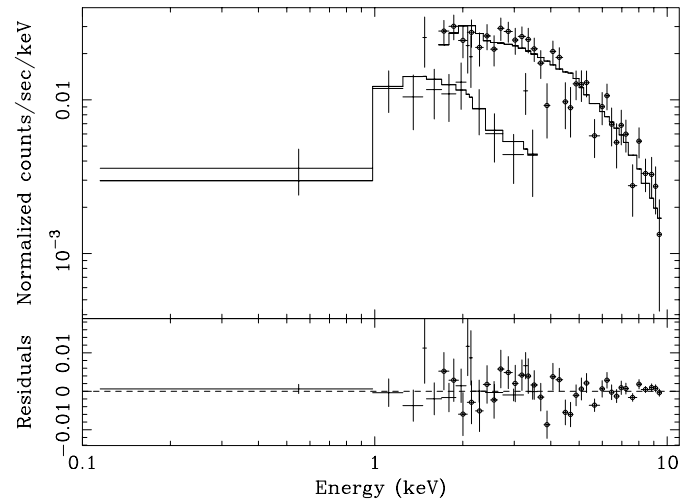


Fig. 5. The LECS and MECS photon spectrum (*upper panel*) and the residuals (*lower panel*) of the pulsed fraction when a power-law with low energy absorption of $N_{\text{H}} = 3.6 \times 10^{21} \text{ cm}^{-2}$ is fitted to the BeppoSAX spectrum.

We also used the PDS data to obtain an upper limit to the pulsed flux in the energy band (13–50 keV) of $9.8 \times 10^{-12} \text{ erg cm}^{-2} \text{ s}^{-1}$, with the confidence of 2σ and assuming a duty cycle of 0.5.

4. Discussion

The measure of the braking index of spinning powered pulsars is important to understand the magnetic field evolution (Muslimov & Page 1996; Ruderman et al. 1998). On the basis of our analysis we confirm that PSR B0540–69 is characterized by a quite low value of n . A smaller value has been reported only for the Vela pulsar (Lyne et al. 1996). Our result is also compatible with 2.08 estimated by Deeter et al. (1998), whereas we can exclude the values > 2.2 . We can use this result to estimate the changing rate of the magnetic moment μ of the neutron star. Assuming a constant moment of inertia, this rate is given by

$$\dot{\mu}/\mu = (n - 3)/2(\dot{\nu}/\nu) \quad (3)$$

and with the above values, we obtain $\dot{\mu}/\mu = 4.3 \times 10^{-12} \text{ s}^{-1}$, which is about 40% greater than that of Crab.

From our data and previous results it is possible to measure the broad band spectral distribution of PSR B0540–69 from the optical to the X-ray band. This spectrum is shown in Fig. 6 where we plotted, together with the BeppoSAX points, the ROSAT spectrum and the optical-UV measurements by Middleditch et al. (1987) and Hill et al. (1997). The locally estimated spectral slopes do not match well: in particular, the optical-UV data indicate a steep spectrum whose extrapolation in the X-ray band would be much lower than the measured fluxes. This fact could be due to the systematic corrections for the interstellar absorption and to the difficult subtraction of the nebular background, but the presence of a steep spectrum component at these frequencies cannot be excluded.

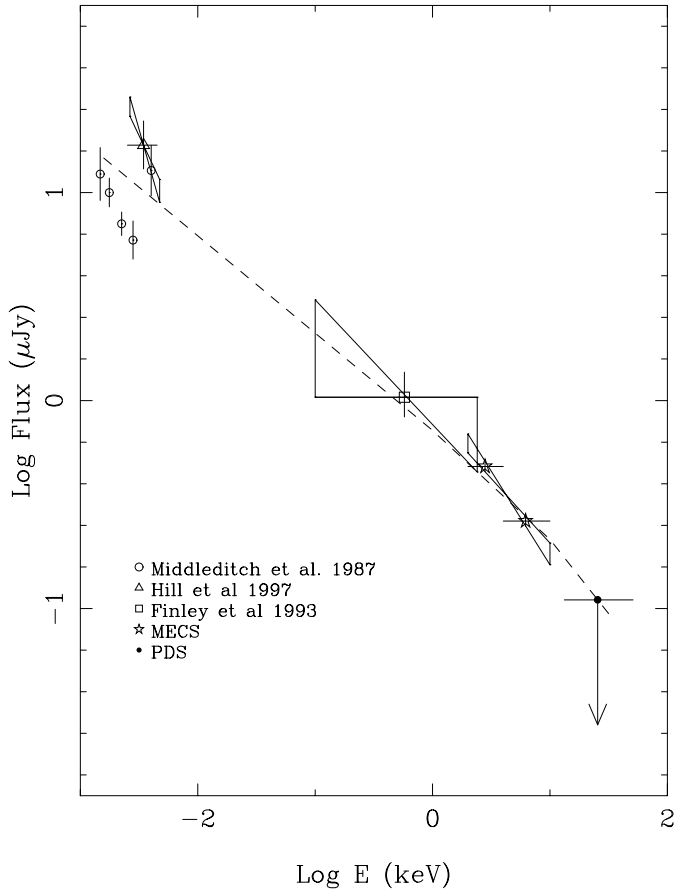


Fig. 6. The energy spectrum of PSR B0540–69 derived from our measurement and from ROSAT (Finley et al. 1993), Middleditch et al. (1987) and Hill et al. (1997) data. The uncertainties on the flux and spectral slope are indicated. The dashed line is the continuum predicted by the Cheng & Wei (1995) model with an energy spectral index of -0.5 .

The origin of the pulsed X-ray emission is still unclear. Cheng & Wei (1995) computed, according to the outer gap model (Cheng et al. 1986a,b), the spectrum of this pulsar assuming that the emission is synchrotron radiation from secondary e^\pm pairs, produced outside the gap by high energy photons. We plot this model spectrum in Fig. 6 (dashed line): it has the energy

slope equal to -0.5 , indicating that only a pair generation is produced, and a cutoff at an energy above 50 keV, higher than our data. At present, the available data are not good enough to allow a precise evaluation of the model parameters. Measurements up to 100 keV with a good statistical quality can probably provide the necessary information for understanding the emission processes in this source.

Acknowledgements. The authors are grateful to M. Ruderman for useful discussions on pulsar models and evolution, and to M.C. Maccarone for the management of the local BeppoSAX SVP data archive. They also acknowledge F.Giambertone for the technical support on data handling. The CNR Institutes and the BeppoSAX Science Data Center are financially supported by the Italian Space Agency (ASI) in the framework of the BeppoSAX mission.

References

- Boella G., Butler R.C., Perola G.C., et al., 1997a, *A&AS* 122, 299
 Boella G., Chiappetti L., Conti G., et al., 1997b, *A&AS* 122, 327
 Boyd P.T., van Citters G.W., Dolan J.F., et al., 1995, *ApJ* 448, 365
 Cheng K.S., Ho C., Ruderman M., 1986a, *ApJ* 300, 500
 Cheng K.S., Ho C., Ruderman M., 1986b, *ApJ* 300, 522
 Cheng K.S., Wei D.M., 1995, *ApJ* 448, 281
 Deeter J.E., Nagase F., Boyton P.E., 1998, in preparation
 Eikenberry S.S., Fazio G.G., Ransom S.M., 1998, *ApJ* 492, 754
 Finley J.P., Ögelman H., Hasinger G., Trumper J., 1993, *ApJ* 410, 323
 Frontera F., Costa E., Dal Fiume D., et al., 1997, *A&AS* 122, 357
 Gouiffes C., Finley J.P., Ögelman H., 1992, *ApJ* 394, 581
 Hill R.J., Dolan J.F., Bless R.C., et al., 1997, *ApJ* 486, L99
 Lyne A.G., Pritchard R.S., Graham-Smith F., Camillo F., 1996, *Nat* 318, 497
 Manchester R.N., Peterson B.A., 1989, *ApJ* 342, L23
 Manchester R.N., Mar D.P., Lyne A.G., Kaspi V.M., Johnston S., 1993, *ApJ* 403, L29
 Manzo G., Giarrusso S., Santangelo A., et al., 1997, *A&AS* 122, 341
 Middleditch J., Pennypacker C.R., 1985, *Nat* 313, 659
 Middleditch J., Pennypacker C.R., Burns M.S., 1987, *ApJ* 315, 142
 Muslimov A., Page D., 1996, *ApJ* 458, 347
 Nagase F., Deeter J., Lewis W., et al., 1990, *ApJ* 351, L13
 Ögelman H., Hasinger G., 1990, *ApJ* 353, L21
 Parmar A.N., Martin D.D.E., Bavdaz M., et al., 1997, *A&AS* 122, 309
 Ruderman M., Zhu T., Chen K., 1998, *ApJ* 492, 267
 Seward F.D., Harnden F.R., Helfand D.J., 1984, *ApJ* 287, L19